Association Between Patellar Tendon Abnormality and Land-Jump Biomechanics in Male Collegiate Basketball Players During the Preseason

Andrew Kraszewski,*† PhD, Erin Argentieri,‡ BS, Kindred Harris,§ MD, Brett Toresdahl,‖ MD, Mark Drakos,† MD, Howard Hillstrom,† PhD, Answorth Allen,† MD, and O. Kenechi Nwawka,† MD

Investigation performed at the Hospital for Special Surgery, New York, New York, USA

Background: Patellar tendinopathy is a degenerative condition that predominantly affects jumping athletes. Symptoms may be subtle or nonexistent at preseason, but structural abnormalities may be present. Assessing patellar tendon abnormality (PTA) through magnetic resonance imaging (MRI) and ultrasound (US) and classifying symptoms using the Victorian Institute for Sport Assessment–Patellar tendon (VISA-P) may provide useful insights if combined with biomechanics measurements.

Purpose: To (1) assess whether land-jump biomechanical patterns are associated with clinically pertinent PTA as seen on imaging and through VISA-P scores and (2) model the contributing risk and accuracy of biomechanics to classify PTA and symptomatic observations.

Study Design: Cross-sectional study; Level of evidence, 3.

Methods: A total of 26 National Collegiate Athletic Association Division I and II male basketball players (n = 52 limbs) were recruited during the preseason. We collected VISA-P scores, bilateral PTA through US and MRI morphology measurements, and bilateral 3-dimensional lower extremity kinematics and kinetics measurements from a land-jump test from an 18-inch-high (45.7-cm-high) box. Statistically, each limb was treated independently. The association of biomechanics with PTA and symptoms (VISA-P score <80) was tested with multivariate models and post hoc tests. Logistic regression modeled relative risk and accuracy of biomechanical variables to classify PTA and symptomatic limbs.

Results: There were 19 to 24 limbs with PTA depending on US and MRI measurements. Differences in hip and knee kinematic strategies and ground-reaction loads were associated with PTA and symptomatic limbs. Peak landing vertical ground-reaction force was significantly decreased (169 $\pm$ 26 vs 195 $\pm$ 29 %body weight; $P = .001$), and maximum hip flexion velocity was significantly increased (416 $\pm$ 74 vs 343 $\pm$ 94 deg/s; $P = .005$) in limbs with versus without PTA on imaging. Knee flexion at the initial contact was decreased in symptomatic versus healthy limbs (17° $\pm$ 5° vs 21° $\pm$ 5°, respectively; $P = .045$). Regression models classified PTA limbs and symptomatic limbs with 71.2% to 86.5% accuracy. Hip and knee maximum flexion velocity and vertical ground-reaction force variables were most common across models observing clinically pertinent PTA.

Conclusion: Our findings suggested that functional kinematic and kinetic biomechanical strategies at the hip and knee were associated with PTA, identified on imaging, and symptomatic limbs.

Keywords: basketball; biomechanics; land-jump; magnetic resonance imaging; patellar tendinopathy; ultrasound

Patellar tendinopathy (PT), also called "jumper's knee," is prevalent among competitive jumping athletes, such as elite basketball players. The prevalence of PT is due to high incidence and recurrence.[23] Reported PT prevalence is 24% in collegiate athletes and over 39% in professional athletes,[14] and PT is twice as prevalent in male athletes compared with female athletes.[32] Frequently, reduced athletic performance and loss of playing time are a result.[4,13] Almost 30% of athletes affected by PT spend up to 6 months recovering.[20]

The Orthopaedic Journal of Sports Medicine, 12(4), 23259671241242008
DOI: 10.1177/23259671241242008

Components of basketball play—such as shooting, rebounding, and other offensive and defensive maneuvers—require repetitive jumping and landing. These put high demands on the knee extensor mechanism and related tissue structures. High-tensile quadriceps loads are borne by the patellar tendon, which transfers force and torque across the knee joint and dissipates kinetic energy.[2] Large forces are magnified in the patellar tendon when the knee is in flexion, and thus, the tendon bears high repetitive stress.

Chronic overloading of the patellar tendon leads to tissue microdamage, and without adequate recovery, damage can accumulate, leading to PT.[21] Structurally, patellar tendon abnormality (PTA) encompasses degenerative changes in the tendon anywhere from the patellar origin to the tibial insertion, which may or may not include tendinitis (inflammation). It can also be asymptomatic clinically.[14] On conventional imaging, magnetic resonance imaging (MRI) and ultrasound (US) are used to visualize tendon morphology and characterize deleterious changes. In addition, it is common to implement survey tools that capture self-reported pain and function. The Victorian Institute of Sport Assessment–Patellar tendon (VISA-P) questionnaire characterizes symptoms, function, and sports-playing ability and is statistically valid.[11,15] However, tendon pathology can be subtle,[3] and examination through conventional imaging does not always correlate with clinical symptoms in asymptomatic athletes.[18] There remains a disconnect between imaging PTA findings and PT symptoms. This is a gap that can be explored by introducing functional assessment.

Landing and jumping movement patterns are commonly associated with PT. Therefore, functional tests that mimic these motions should theoretically elicit changes in biomechanics related to PT presence. Yet, despite numerous studies over the past three decades investigating the link between dynamic function and PT symptoms, there is still limited conclusive evidence.[1,9,24,25] A recent review article has recommended continuing to investigate the link between movement patterns and PT, along with the inclusion of sonographic measurements.[24] The combination of biomechanics, PTA on imaging, and symptom measurements would be novel—to our knowledge, this approach has not been scientifically explored.

Our goal was to explore the association of both clinically pertinent PTA as seen on imaging and symptom metrics with functional biomechanical strategies in elite male basketball players in the preseason. We believe in-season detection is suboptimal and may allow existing patellar tendon damage to accumulate and progress to advanced stages.[21] Therefore, there is a need for earlier PTA detection. Our aims and hypothesis in this study were as follows:

1. Assess the association of PTA on imaging and symptoms with land-jump biomechanical variables. We hypothesized that $\geq$1 lower extremity hip, knee, and ankle joint strategy would be different in limbs with radiologic PTA and self-reported symptoms compared with healthy limbs.
2. Model the relative risk and accuracy of biomechanical variables to classify both PTA and symptoms. We hypothesized that lower extremity hip, knee, and ankle joint strategies would strongly classify limbs with radiologic PTA and symptoms.

METHODS

Participant Recruitment

This study was a cross-sectional analysis of the preseason of a longitudinal timepoint investigation. The target sample size was 40 participants. We employed MRI and US measurements to identify PTA on imaging and used the VISA-P to identify symptoms. We then quantified function with lower extremity kinematics and kinetics during a land-jump test, focusing on the sagittal plane of movement.

The protocol for this study received ethical approval from our institutional review board. Local area National Collegiate Athletic Association (NCAA) Division I and II collegiate male basketball teams were recruited through their coach or athletic medical staff. Players with a previous surgery involving the knee, a previous injection of the knee extensor mechanism, a history of diabetes, a history of a connective tissue disorder, or a current pathology affecting the ability to jump or land were excluded. Participants were not screened for PTA or symptoms before entering the study. All study participants provided written informed consent.

Clinical Assessment: VISA-P

Study staff administered the VISA-P questionnaires electronically during the preseason visit. The questionnaire

*Address correspondence to Andrew Kraszewski, PhD, Leon Root, MD Motion Analysis Laboratory, 510 East 73rd Street, New York, NY 10021, USA (email: andrew.kraz@gmail.com).
†Hospital for Special Surgery, New York, New York, USA.
‡University of California–Berkeley, Berkeley, California, USA.
§University of Arizona College of Medicine, Tucson, Arizona, USA.
‖University of Utah Health, Salt Lake City, Utah, USA.
Final revision submitted August 10, 2023; accepted August 29, 2023.
One or more of the authors has declared the following potential conflict of interest or source of funding: Financial support was received from a National Basketball Association/GE Healthcare Orthopedics and Sports Medicine Collaboration grant. M.D. has received education payments from Gotham Surgical; nonconsulting fees from Arthrex; consulting fees from Extremity Medical and DePuy Synthes; and royalties from Extremity Medical. H.H. is the CTO of Biomed Consulting, and his spouse is the CEO of Biomed Consulting. A.A. has received education payments and consulting fees from Arthrex. O.K.N. has received nonconsulting fees from GE Healthcare and consulting fees from Canon Medical Systems USA. AOSSM checks author disclosures against the Open Payments Database (OPD). AOSSM has not conducted an independent investigation on the OPD and disclaims any liability or responsibility relating thereto.
Ethical approval for this study was obtained from the Hospital for Special Surgery (reference No. 2016-627).

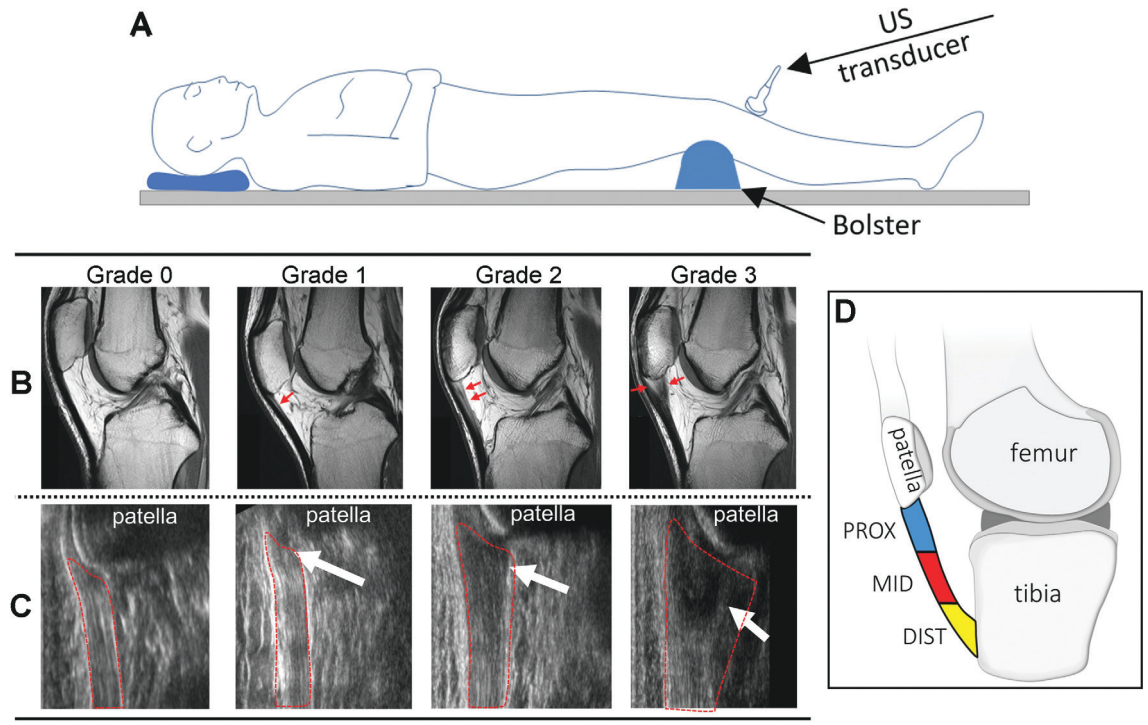

Figure 1. (A) Illustration of a patient in the supine position for the MRI and US measurements. (B) Sagittal MRI images of knees representing each morphology (grades 0-3) in the proximal tendon region. (C) US images of knees representing each morphology (grade 0-3) in the proximal tendon region. Red and white arrows indicate areas of patellar tendon degeneration. The tendon is inside the areas outlined by red dashes. (D) Illustration of the knee joint showing major structures and proximal and distal regions of the patellar tendon. DIST, distal; MID, medial; MRI, magnetic resonance imaging; PROX, proximal; US, ultrasound.

consists of 8 questions related to pain and function, each scored 0 to 10, with 0 indicating severe pain or dysfunction and 10 indicating no pain or dysfunction. The scores for all questions are summed to give a total score from 0 to 80. A higher score indicates better patellar tendon health and less pain and dysfunction, while a lower score suggests more severe symptoms and impaired function.

Clinical Imaging Measurements

All MRI and US measurements were performed by a fellowship-trained, expert, board-certified musculoskeletal radiologist with over 9 years of clinical experience (O.K.N.).

Magnetic Resonance Imaging. Bilateral 2-dimensional multiplanar fast-spin echo MRI sequences were utilized for clinical morphologic MRI evaluation of the tendon using a 3.0-T MRI scanner (DV 750; GE Healthcare) and an 8-channel phased array knee coil (echo time: 25 ms, repetition time: 4000 ms, number of excitations: 2, receiver bandwidth: ± 62.5 kHz, field of view: 14-16 cm, slice thickness: 3.5 mm, matrix: 512 × 384 mm). The imaging physician reviewing the MRI data, who was an experienced attending radiologist but not a study investigator, was blinded to the US evaluation.

Ultrasound. Bilateral morphologic US measurements were obtained. Each participant was placed in a supine position with a wedge immobilizer under the evaluated knee to maintain a constant 20° of knee flexion (Figure 1A), per the American Institute of Ultrasound in Medicine and the American College of Radiology recommendations. US evaluations used a 9-MHz transducer on a LOGIQ E9 US system (GE Healthcare). The imaging physician (O.K.N.) reviewing the US data was blinded to the MRI evaluation.

Imaging Variables

Morphologic PTA measurements were taken in a region-specific manner and graded using a 4-point qualitative scale: 0 (normal), 1 (<33%, mild), 2 (33%-67%, moderate), and 3 (>67%, severe). Proximal and distal regions were assessed (Figure 1B). Grading on the US was based on the percentage of abnormal tendon echogenicity and morphology—including fissuring, thickening, and tearing). For MRI, the radiologist graded PTA based on the percentage volume of the abnormal signal on axial moderate echo time acquisitions.

Dynamic Land-Jump Measurements

Testing Protocol and Environment. A box-to-ground-to-box jump (land-jump) task was performed in an instrumented motion analysis laboratory. The land-jump task

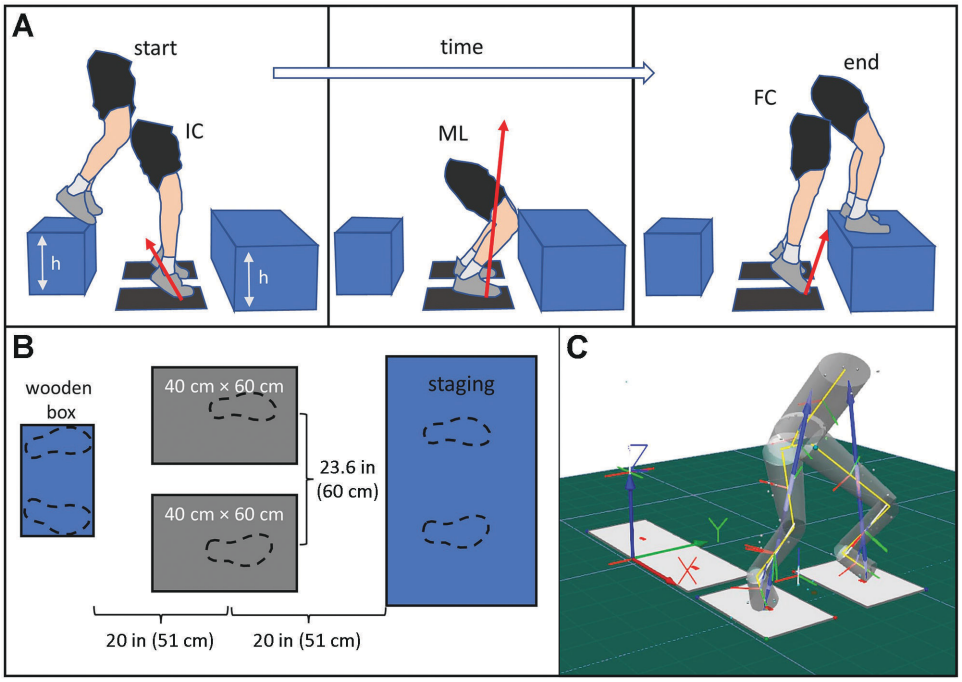

Figure 2. Physical dimensions and arrangement of the land-jump test. (A) Illustration of the dynamic land-jump task at initial contact, midlanding, and final contact, with platform and force plate objects drawn to scale. The platform h was 18 inches (45.7 cm). The red arrow depicts a ground-reaction force vector. (B) A diagram from a top-down perspective of the physical arrangement for the wooden box, force plates, and staging platform; the foot placement depicted as dashed lines is approximate. (C) A frame from the 3-dimensional motion reconstruction program (Visual3D, Version 6; C-Motion) showing the virtual world and rigid-body model near the ML event along with blue ground-reaction force vector arrows. Note: the 2 adjacent force platforms in the immediate background were not used. IC, initial contact; ML, midlanding; FC, final contact; h, height.

consisted of jumping forward and down from a wooden box, landing on force plates, and immediately jumping up to a platform in front (Figure 2). Two 40 × 60-cm force plates (Bertec) were aligned in parallel 0.6 m apart with respect to each plate's long axis. An 18-inch (45.7-cm) tall × 12-inch (30.5-cm) wide × 18-inch (45.7-cm) long wooden exercise box was aligned centrally with the force plates, and its closest edge was positioned 20 inches (50.8 cm) from the middle short axes of the plates. An 18-inch (45.7-cm) tall × 36-inch (91.4-cm) long × 36-inch (91.4-cm) wide platform was aligned centrally; its closest edge was positioned 20 inches (50.8-cm) horizontally from the middle short axes of the plates.

Double-sided adhesive tape was used to affix 10-mm diameter retroreflective motion capture markers to the skin over bony landmarks based on the International Society of Biomechanics anatomical coordinate frame recommendations.[30] In addition, 4-marker clusters with a rigid plastic base were attached over the skin to the thigh and shank segments distally with elastic wrap (Coban; 3M).

Participants were instructed to perform the land jump in a continuous motion without pausing during the landing and while trying to maintain their foot position within the bounds of the respective force plates. Athletes were allowed several practice repetitions to familiarize themselves with the task and ensure all concerns were addressed. Before the first jump, athletes were asked to carefully mount and stand on the wooden box and wait for a verbal cue to proceed. A short static trial was recorded with the participant standing in a T-pose with arms extended and abducted to 90° and feet positioned a hip-width apart. After that, 10 land jumps per athlete were recorded for analysis.

Participants were recorded with a 12-camera optical motion capture system (Motion Analysis Corp) calibrated with 0.4 mm residual errors. Marker positions were recorded at 200 frames per second, and limb ground-reaction loads were synchronized and recorded at 1000 frames per second.

Motion Data Processing. Marker identification and tracking were performed with commercial software (Cortex version 7; Motion Analysis Corp). Signal processing, model building, and 3-dimensional motion reconstruction were performed with commercial software (Visual3D, Version 6; C-Motion). Marker trajectories were low-pass filtered with a fourth-order zero-lag Butterworth algorithm at a 15.0-Hz cutoff. Subject-scaled rigid-body models were built from static trial marker data with assumed prismatic joints at the hip (ball-and-socket), knee (saddle), and ankle (ball-and-socket). Default segment tracking weight factors for the pelvis, thighs, shanks, and feet were 5.0, 2.0, 3.0, and 5.0, respectively. Inverse kinematics employed a quasi-Newton optimization with simulated annealing to solve a least-squares global model pose at each frame.

TABLE 1
List of Biomechanical and Imaging Variables Used, With Units of Measure and Definitions[a]

Variables	Unit	Definition
Biomechanical variables		
Peak VGRF time	cs	Time from IC to IP-VGRF in centiseconds
Peak landing VGRF	%BW	VGRF value taken at IP-VGRF, normalized by mass
Peak jumping VGRF	%BW	Peak VGRF during jumping phase, normalized by mass
VGRF impulse	%BW·s	VGRF impulse during contact, normalized to % bodyweight
Knee flexion impulse	$m^2 \cdot g/s$	Knee angular impulse in sagittal plane, normalized by mass/*g*
Maximum knee extension torque	$m^2 \cdot g/s^2$	Peak landing knee extension torque, normalized by mass/*g*
Maximum eccentric knee power	m^2/s^3	Peak eccentric knee flexion power, normalized to mass
Maximum concentric knee power	m^2/s^3	Peak concentric knee flexion power, normalized to mass
Hip flexion at IC	deg	Hip flexion angle taken at IC
Hip flexion at IP-VGRF	deg	Hip flexion angle taken at IP-VGRF
Maximum hip flexion	deg	Maximum hip flexion angle
Hip flexion velocity at IC	deg/s	Hip flexion angular velocity taken at IC
Maximum hip flexion velocity	deg/s	Maximum hip flexion angular velocity during landing
Hip flexion velocity at IP-VGRF	deg/s	Hip flexion angular velocity taken at IP-VGRF
Knee flexion at IC	deg	Knee flexion angle taken at IC
Knee flexion velocity at IC	deg/s	Knee flexion angular velocity taken at IC
Maximum knee flexion velocity	deg/s	Maximum knee flexion angular velocity during landing
Knee flexion at IP-VGRF	deg	Knee flexion angle taken at IP-VGRF
Maximum knee flexion	deg	Maximum knee flexion angle
Knee flexion velocity at IP-VGRF	deg/s	Knee flexion angular velocity taken at IP-VGRF
Ankle flexion at IC	deg	Ankle (shoe-to-shank) flexion angle taken at IC
Ankle flexion velocity at IC	deg/s	Ankle flexion angular velocity taken at IC
Maximum ankle flexion velocity	deg/s	Maximum ankle flexion angular velocity during landing
Ankle flexion at IP-VGRF	deg	Ankle flexion angle taken at IP-VGRF
Ankle flexion velocity at IP-VGRF	deg/s	Ankle flexion angular velocity taken at IP-VGRF
Maximum ankle flexion	deg	Peak ankle flexion angle
Imaging variables		
MRI_{PROX}	grade	Patellar tendon morphology grade near patella, based on MRI
MRI_{DIST}	grade	Patellar tedon morphology grade near tibia, based on MRI
US_{PROX}	grade	Patellar tendon morphology grade near patella, based on US
US_{DIST}	grade	Patellar tendon morphology grade near tibia, based on US
Symptom variable		
VISA-P	point	Cumulative value of ranked self-reported questionnaire items

[a]BW, body weight; DIST, distal patellar tendon region; *g*, gravity (9.806 m/s^2); IC, initial contact; IP-VGRF, initial peak vertical ground-reaction force; MRI, magnetic resonance imaging; PROX, proximal patellar tendon region; US, ultrasound; VISA-P, Victorian Institute for Sport Assessment–Patellar tendon; VGRF, vertical ground-reaction force.

Then, additional low-pass Butterworth filters smoothed noise introduced by the pose optimization: pelvis (8.0 Hz), thighs (8.0 Hz), shank (8.0 Hz), and feet (10.0 Hz). The mean pose tracking residual error was kept at <3 cm, and occasionally, segment weight factors were adjusted to meet this criterion. The body mass was measured with force plates, and kinetic signals were normalized to either body mass (kg) or body weight (% body weight [BW]). The first and last trials and any outliers were excluded based on the visual analysis of the vertical ground-reaction forces (VGRFs). Excluded trials were those where 1 or both of the athlete's feet landed off a force plate, seen as a grossly underestimated or misaligned force signal, or the investigator suspected a pause, seen as a clear "double-hump" pattern in the vertical force signal. Five to 8 trials were averaged for analysis.

A total of 31 variables (26 biomechanical, 4 MRI and US, and 1 VISA-P) were considered (Table 1). All biomechanical variables were calculated during ground contact, where "contact" was defined as the point at which the total (whole body) VGRF exceeded 10 N. The land jump was split into 2 phases: landing and jumping. Landing was defined as the time from the initial contact (IC) to the moment of lowest pelvis vertical height, and jumping was defined as the rest of the time to the final contact. The initial peak VGRF (IP-VGRF) event was defined as the largest local maxima during the landing phase and was calculated per limb.

Statistical Analysis

Biomechanical variables were averaged across trials to represent each participant; each participant had 2 limb observations per variable; all limbs were treated as independent observations. Morphological PTA measurements were collapsed into a binary variable of "no PTA" (grade = 0) or "PTA" (grade $\geq$ 1). Player VISA-P observations were categorized as either "healthy" (VISA-P $\geq$ 80) or

TABLE 2
Demographic Characteristics of the Preseason Cohort Stratified by the Presence of PTA[a]

	All Players (N = 26)	No PTA Any Limb (n = 7)	PTA Single Limb (n = 10)	PTA Both Limbs (n = 9)
Age, y	19.7 ± 1.1	19.3 ± 1.3	20.1 ± 1.2	19.6 ± 0.7
Height, cm	194.4 ± 9	192 ± 8	193.3 ± 9	197.6 ± 9.9
Weight, kg	89.7 ± 11.4	86.9 ± 8.5	91.1 ± 13.7	93.3 ± 14.2
BMI, kg/m^2	23.9 ± 2.6	23.6 ± 1.8	24.3 ± 2.6	23.9 ± 3.4
Class				
Freshman	8 (31)	2 (28)	3 (30)	3 (33)
Sophomore	9 (35)	4 (57)	2 (20)	3 (33)
Junior	5 (19)	0 (0)	3 (30)	2 (22)
Senior	4 (15)	1 (14)	2 (20)	1 (11)
Position				
Forward	8 (31)	1 (14)	3 (30)	4 (44)
Guard	16 (62)	5 (71)	7 (70)	4 (44)
Center	2 (7)	1 (14)	0 (0)	1 (11)
VISA-P score	90.3 ± 10.4	93.3 ± 6.8	89.8 ± 10.6	88.4 ± 12.7

[a]Data are reported as mean ± SD or n (%). PTA was defined as the mean morphology grade across all 4 MRI and US imaging variables rounded to the nearest grade, where 0 indicated no PTA and ≥1 indicated PTA. BMI, body mass index; MRI, magnetic resonance imaging; PTA, patellar tendon abnormality; US, ultrasound; VISA-P, Victorian Institute for Sport Assessment–Patellar tendon.

"symptomatic" (VISA-P < 80) using a cutoff commonly found in the literature.[6,10,15,29] Bilateral measurements were analyzed per player.

Aim 1. Association of Biomechanical Strategies With PTA and Symptoms. Multivariate analysis of variance (MANOVA) models tested the effect of PTA (MRI_{PROX} and US_{PROX} and MRI_{DIST} and US_{DIST}) and symptoms variables on grouped biomechanical variables. Lower limb dominance was also included as a model factor. Separate MANOVA models were fit using biomechanical variables grouped in several ways: (1) 3 joint flexion kinematics groups per the hip, knee, and ankle (flexion at IC, flexion at IP-VGRF, maximum flexion, flexion velocity at IC, flexion velocity at IP-VGRF, maximum flexion velocity); (2) knee flexion kinetics (knee flexion impulse, peak knee extension torque, peak concentric knee power, and peak eccentric knee power); and (3) VGRF kinetics (peak VGRF time, peak landing VGRF, peak jumping VGRF, and VGRF impulse). The statistical criterion was the Wilk lambda. Only statistically significant MANOVAs were followed by post hoc contrasts and univariate tests if indicated.

Aim 2. Classification and Risk Modeling of PTA and Symptoms With Biomechanical Metrics. Logistic regression was employed to classify PTA and symptomatic limb events and quantify risk with odds ratios. Given a large pool of candidate biomechanical variables, the challenge was to find a model that maximized the total classification rate and goodness of fit. To avoid overfitting, a maximum of 3 predictors (k) not including the intercept were allowed per outcome,[28] then all combinations of models with k predictors out of 26 were fit to create a sample totaling $\frac{26!}{k!(26-k)!}$ models associated with each outcome. Classification rate (%) and modified Akaike information criterion (AIC) were recorded. From each outcome sample of models, a single model was chosen based on 3 criteria: first, both high overall classification rates and low AIC values then, in ambiguous cases, high positive event classification rates. Classification was judged as poor (0%-40%), marginal (41%-65%), good (66%-85%), or excellent (86%-100%).

The robustness of each chosen regression model was assessed with a bootstrap procedure. Bootstrapping was performed by resampling the regression coefficients with an iterative leave-*N*-subjects-out procedure. Per iteration, approximately 30% of the total limb observations were excluded, where a participant's paired limbs were removed and never single limbs. This sampling procedure produced estimates for each variable through median odds ratios and percentile-based 95% CIs, as well as median overall percentage accuracies with percentile-based 95% CIs.

Statistical significance was set at $P < .05$. All statistics were performed in MATLAB with the Statistics and Machine Learning Toolbox (Version 2021b; MathWorks) and the Real Statistics package for Microsoft Excel.[31]

RESULTS

A total of 27 male NCAA collegiate athletes from 4 Northeast Coast basketball teams were recruited and enrolled between 2016 and 2019. One athlete opted out of the study, and his data were excluded from the analysis. Fifteen participants were from NCAA Division I and 11 from Division II schools. All players were consented and tested during the preseason months ranging from August to October. Stratified demographic information is shown in Table 2. The VISA-P scores for 4 athletes were categorized as symptomatic (71.3 ± 7.1 [range, 61-76]), and the scores for 22 athletes were categorized as healthy (93.7 ± 6.3 [range, 82-100]).

Both MRI and US morphology observations were predominantly grades 0 (55%) or 1 (30%) and sparsely grades 2 (13%) or 3 (2%). Therefore, the operational definition of PTA in this study was the presence (grade >0) or absence (grade = 0) of PTA on imaging—a binary variable.

TABLE 3
Results From the Multivariate Analysis of Variance[a]

	Independent Variable			
	MRI_{PROX}			
Dependent Variable	PTA (n = 19)	No PTA (n = 33)	Difference	*P*
Hip flexion kinematics				<.001[b]
Hip flexion at IC	29 ± 12	33 ± 6	–4 ± 2	
Hip flexion at IP-VGRF	49 ± 9	49 ± 8	0 ± 2	
Maximum hip flexion	73 ± 14	71 ± 17	1 ± 5	
Hip flexion velocity at IC	80 ± 81	96 ± 76	–16 ± 22	
Maximum hip flexion velocity	**416 ± 74**	**343 ± 94**	**73 ± 25**	
Hip flexion velocity at IP-VGRF	373 ± 91	320 ± 98	54 ± 27	
VGRF kinetics				.030[b]
Peak VGRF time	7.5 ± 1.8	6.9 ± 1.6	0.6 ± 0.5	
Peak landing VGRF	**169 ± 26**	**195 ± 29**	**–27 ± 8**	
Peak jumping VGRF	140 ± 13	155 ± 34	–15 ± 8	
VGRF impulse	483 ± 55	481 ± 85	2 ± 22	
	US_{PROX}			
	PTA (n = 20)	No PTA (n = 32)		
Hip flexion kinematics				.041[b]
Hip flexion at IC	30 ± 11	32 ± 7	–2 ± 2	
Hip flexion at IP-VGRF	49 ± 9	49 ± 8	0 ± 2	
Maximum hip flexion	71 ± 13	73 ± 18	–2 ± 5	
Hip flexion velocity at IC	87 ± 85	92 ± 73	–4 ± 22	
Maximum hip flexion velocity	401 ± 90	350 ± 92	51 ± 26	
Hip flexion velocity at IP-VGRF	367 ± 93	322 ± 98	45 ± 27	
	VISA-P Score			
	Symptomatic (n = 8)	Healthy (n = 44)		
Knee flexion kinematics				.033[b]
Knee flexion at IC	**17 ± 5**	**21 ± 5**	**–4 ± 2**	
Knee flexion at IP-VGRF	55 ± 4	55 ± 9	0 ± 3	
Maximum knee flexion	87 ± 11	83 ± 11	4 ± 4	
Knee flexion velocity at IC	225 ± 62	203 ± 117	22 ± 43	
Maximum knee flexion velocity	598 ± 55	568 ± 82	30 ± 30	
Knee flexion velocity at IP-VGRF	531 ± 80	475 ± 129	56 ± 47	

[a]Data are reported as mean ± standard error. See Table 1 for units of measure associated with the biomechanical variables. Bolded rows indicate significant differences according to univariate analysis of variance ($P < .05$). IC, initial contact; IP-VGRF, initial peak vertical ground-reaction force; MRI, magnetic resonance imaging; PROX, proximal patellar tendon region; PTA, patellar tendon abnormality; US, ultrasound; VISA-P, Victorian Institute for Sport Assessment–Patellar tendon; VGRF, vertical ground-reaction force.
[b]Statistically significant difference ($P < .05$).

Association of Patellar Morphology With Biomechanical Variables

Two-way MANOVA models were fit with 52 limb observations per biomechanical dependent variable against each of the 4 MRI and US PTA variables and the VISA-P symptoms variable. All MANOVA models are presented in Supplemental Tables S1 to S5 (available separately). Five models were significant with respect to PTA and symptoms (Table 3). Limb dominance was not a significant factor. A significant effect of PTA as measured by MRI_{PROX} was found in the hip flexion kinematics group ($F = 5.13$; $P < .001$) and the VGRF kinetics group ($F = 3.50$; $P = .030$). A significant effect of PTA as measured by US_{PROX} was found in the hip flexion kinematics group ($F = 2.42$; $P = .041$). A significant effect of VISA-P symptoms was observed with the knee flexion kinematics group ($F = 2.54$; $P = .033$).

Follow-up univariate tests indicated that peak landing VGRF was significantly decreased (169 ± 26 vs 195 ± 29 % body weight (%BW); $P = .001$) and maximum hip flexion velocity was significantly increased (416 ± 74 vs 343 ± 94 deg/s; $P = .005$) for MRI_{PROX} PTA versus no-PTA limbs. In

TABLE 4
Results of Binomial Logistic Regressions[a]

	Selected Best Model				Bootstrap[d]	
Outcome and Variables	$P_{Variable}$	OR (95% CI)[b]	% Accuracy	P_{Model}[c]	OR[e]	% Accuracy[e]
MRI_{PROX}			84.6	**<.001**		84.6 (76-88.5)
Maximum hip flexion	.027	0.92 (0.85-0.99)			0.92 (0.84-0.96)	
Maximum hip flexion velocity	.003	1.02 (1.01-1.04)			1.02 (1.01-1.03)	
Peak landing VGRF	.005	0.96 (0.93-0.99)			0.96 (0.90-0.98)	
MRI_{DIST}			73.1	.057		67.3 (57.7-73.1)
Maximum hip flexion velocity	.177	1.01 (1-1.01)			1.01 (1-1.02)	
Knee flexion at IC	.034	1.15 (1.01-1.31)			1.15 (1.03-1.37)	
Maximum knee flexion	.032	0.92 (0.85-0.99)			0.92 (0.80-0.97)	
US_{PROX}			82.7	**.001**		80.8 (73.1-84.6)
Maximum hip flexion	.011	0.90 (0.83-0.98)			0.90 (0.7-0.94)	
Hip flexion velocity at IP-VGRF	.006	1.02 (1-1.03)			1.02 (1.01-1.04)	
Peak landing VGRF	.013	0.97 (0.94-0.99)			0.96 (0.92-0.98)	
US_{DIST}			71.2	**.042**		67.3 (57.7-73.1)
Hip flexion velocity at IC	.045	1.01 (1-1.02)			1.01 (1-1.03)	
Knee flexion velocity at IC	.216	1 (0.99-1)			0.99 (0.99-1)	
Maximum knee flexion velocity	.052	0.99 (0.98-1)			0.99 (0.98-1)	
VISA-P			86.5	**.030**		
Knee flexion at IC	.052	0.83 (0.69-1.00)				

[a]All the best 3-variable models were based on low modified Akaike information criterion values and high accuracy. For units of measure associated with the biomechanical variables, see Table 1. DIST, distal patellar tendon region; IC, initial contact; IP-VGRF, initial peak vertical ground-reaction force; MRI, magnetic resonance imaging; OR, odds ratio; PROX, proximal patellar tendon region; PTA, patellar tendon abnormality; US, ultrasound; VISA-P, Victorian Institute for Sport Assessment–Patellar tendon; VGRF, vertical ground-reaction force.

[b]Odds ratio is the relative change in odds ($P/(1-P)$) of observing a PTA or symptomatic limb per unit increase in the variable, holding other model variables constant at a mean value.

[c]P (χ^2 test) is based on the deviance test that compares with an intercept-only model.

[d]Estimated with bootstrap by sampling over all leave-8-out combinations.

[e]Median (95% CI), with 95% CI based on bootstrap sample 2.5% and 97.5% percentiles.

US_{PROX} PTA limbs, no individual hip flexion kinematic variables were statistically significant. Decreased knee flexion at the IC was observed in symptomatic versus healthy VISA-P limbs (17° ± 5° vs 21° ± 5°; $P = .045$).

Classifying PTA and Symptoms With Biomechanics

Imaging PTA and symptoms models used 52 limb observations. PTA group sizes indicated a maximum of 3 biomechanical predictor variables, and the symptoms group size indicated a single predictor. A sample of 2600 different 3-variable binomial logistic regression models were fit per imaging PTA outcome, and 26 single-variable models fit VISA-P symptoms. The best model per outcome was based on classification accuracy and AIC (Supplemental Figure S1). All odds ratios were expressed with respect to the no-PTA and healthy categories. Limb observations from eight (30.8%) different participants were excluded per iteration to perform bootstrapping, but all possible combinations totaled more than 1,500,000 models; thus, instead, 40,000 were randomly selected. Imaging PTA models were bootstrapped, but VISA-P symptoms models were not given because there were only 8 symptomatic limb observations.

Three out of four selected regression models (Table 4) were statistically significant, with overall accuracy from 71.2% to 86.5%. The best MRI_{PROX} model ($P < .001$) was overall 84.6% accurate (no PTA: 87.9%; PTA: 78.9%), with all 3 statistically significant variables confirmed with bootstrapping. The best MRI_{DIST} model ($P = .057$) was overall 73.1% accurate (no PTA: 90.3%; PTA: 47.6%), with 2 statistically significant variables confirmed with bootstrapping. The best US_{PROX} model ($P = .001$) was overall 82.7% accurate (no PTA: 90.6%; PTA: 70%), with all 3 significant variables confirmed with bootstrapping. The best US_{DIST} model ($P = .042$) was overall 71.2% accurate (no PTA: 82.1%; PTA: 58.3%), with 1 statistically significant variable confirmed with bootstrapping. The best VISA-P model ($P = .030$) was overall 86.5% accurate (healthy: 100%; symptomatic: 12.5%), without a significant variable. Contributions of individual biomechanical variables to the probability of observing PTA in a limb can be seen in Supplemental Figure S2 (available separately).

The most common biomechanical variables among the intersecting models in terms of 95th percentile AIC and 95th percentile accuracy are shown in Figure 3. The 5 most common variables were maximum hip flexion velocity, maximum knee flexion velocity, peak landing VGRF, hip flexion velocity at IP-VGRF, and VGRF impulse. Maximum hip flexion velocity increased the probability of observing PTA from 1 to 1.02 times per 1 deg/s increase. There was moderate agreement of odds ratios between

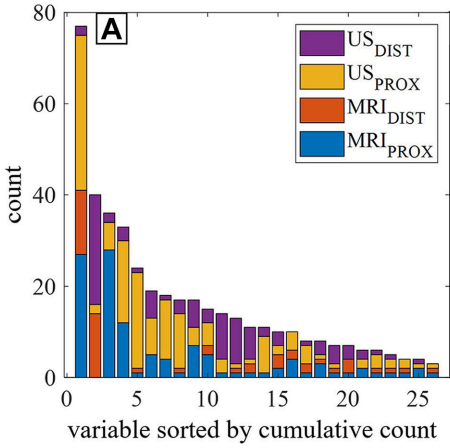

		MRI_{PROX}	MRI_{DIST}	US_{PROX}	US_{DIST}
1.	maximum hip flexion velocity	1.015	1.006	1.014	0.996
2.	maximum knee flexion velocity	--	0.989	0.994	0.991
3.	peak landing VGRF	0.961	--	0.973	--
4.	hip flexion velocity at IP-VGRF	1.023	--	1.016	1.005
5.	VGRF impulse	0.996	1.000	0.986	1.005
6.	peak VGRF time	3.06	--	1.739	0.606
7.	maximum hip flexion	0.913	--	0.930	1.020
8.	maximum eccentric knee power	0.940	1.000	0.800	1.063
9.	knee flexion velocity at IP-VGRF	0.980	--	0.993	0.991
10.	knee flexion velocity at IC	0.994	0.995	0.996	0.994

Figure 3. Details of intersecting 95th percentile regression model variables. (A) A stacked bar chart shows the individual and cumulative count of biomechanical variables per PTA outcome. (B) List of the top 10 cumulative variables and corresponding mean odds ratios per PTA outcome. The odds ratios were evaluated in each model with 2 other variables present. The VISA-P outcome was not shown because all regression models contained a single variable. See Table 1 for units of measure associated with the biomechanical variables. DIST, distal patellar tendon region; IC, initial contact; IP-VGRF, initial peak vertical ground-reaction force; MRI, magnetic resonance imaging; PROX, proximal patellar tendon region; PTA, patellar tendon abnormality; US, ultrasound; VGRF, vertical ground-reaction force; VISA-P, Victorian Institute for Sport Assessment–Patellar tendon; dashes indicate no data.

PTA outcomes, with poor agreement in particular for the peak VGRF time variable. The least frequent variable was ankle flexion velocity at IP-VGRF.

DISCUSSION

We found evidence that land-jump biomechanics measurements were associated with PTA and symptoms. Our strongest kinematic findings was a significant association of PTA limbs with increased maximum hip flexion velocity (MRI_{PROX} PTA vs no-PTA limbs: 416 ± 74 vs 343 ± 94 deg/s; $P = .005$). Generally, these results aligned with evidence reported by Tayfur et al.[24] We speculate this behavior may be a proximal compensation strategy to indirectly decrease patellar loading by altering the trunk, pelvis, and hip deceleration.

There was also strong kinetic evidence that peak landing VGRF was significantly decreased in PTA limbs (MRI_{PROX} PTA vs no-PTA limbs: 169 ± 26 vs 195 ± 29 %BW; $P = .001$). Combined with longer peak VGRF times on average (although not significant), this aligns with findings by Harris et al,[10] who found that basketball players with PTA had decreased loading rates from contact to peak vertical force. In addition, we noted decreased variability in the VGRF curves throughout ground contact and speculate this is a strategy adopted to protect the limb; this type of coordination strategy has been previously reported to be associated with overuse injuries.[7] We observed less knee flexion at the IC and greater maximum knee flexion—translating into a greater range of motion—which allows more time to decelerate, thereby decreasing loading rates and peak loads in PTA limbs. The knee extensor torque has been reported to decrease[5,22] and increase[10] in minimally symptomatic and asymptomatic PT groups, in which the former result agrees with our general findings. Other knee flexion kinetics were decreased on average in affected limbs, such as lower peak eccentric landing power; this could be partially explained by the decrease in VGRF magnitude and the longer duration to peak landing VGRF observations.

A systematic review by Harris et al[9] identified 37 biomechanical variables from 13 cross-sectional and prospective PT studies. They concluded that no crucial biomechanical variable associated with PT was found, although they did note 2 variables, namely, knee flexion at IC and hip extension during horizontal landing, were replicated between 2 studies investigating asymptomatic patellar abnormality. A recent review and meta-analysis by Tayfur et al[24] identified 16 studies and scrutinized kinematic and kinetic results for evidence of association between PT and landing biomechanics. They found moderate evidence supporting reduced knee power in players with PT, which was consistent with our main findings. They also found strong evidence for a lack of association between knee flexion torque and PT, which we feel disagrees with our findings. Both reviews pointed to a lack of uniformity across the literature and critiqued those past studies that utilized cross-sectional designs and were heterogeneous, mainly with respect to cohort selection and the specific experimental task. These cohorts included competitive volleyball, handball, korfball, and basketball players, as well as recreational athletes and dancers; only 1 study exclusively studied basketball athletes of "subelite" status.[15] Those inclusive of basketball athletes examined vertical stop-jumps with horizontal landing[10,15] and 50-cm drop landings.[22] Our test had both a drop landing and vertical jump components, but it lacked a running and lateral stop component.

The VISA-P scores in the patients with PTA were relatively healthy considering, for example, athletes with PT (64 ± 17.2) among collegiate sports clubs from Kregel et al[12] and among volleyball players[27] (76 ± 12) and

jumping athletes (72 ± 22) from Visnes et al.[26] This is not that surprising, given those and other studies based PT determination largely on pain, which is a primary dimension of the VISA-P tool. The finding lends further credence to the disagreement between diagnostic imaging and self-reported symptom scores.

Classifying PTA and VISA-P With Biomechanical Variables

The imaging PTA regression models performed well and were generally robust, which suggests that biomechanical metrics have a potential role in screening athletes. In the top 5% of PTA models, the more frequent variables generally aligned with our MANOVA findings, as expected. The estimated odds ratios had mixed agreement and, in 1 instance, very different values across PTA outcomes. We speculate that imaging modality and the patellar tendon region may have other relationships with lower extremity biomechanics. Few studies have reported using biomechanical metrics to classify or assign risk to clinically pertinent PT. An early comparative study by Richards et al[19] measured the 3-dimensional biomechanics of jumping in 11 volleyball players, and they reported that positive predictors of patellar tendinitis pain were increased knee flexion and increased peak VGRF. The first corroborated our results but not the second; thus, explaining both the agreement and tension is challenging given the differences in numerous aspects of the study design and methodology. In other prospective work, Visnes et al[26] found that greater countermovement jump height was a significant predictor (odds ratio, 2.09 [95% CI, 1.03-4.25]) of developing symptomatic PT in volleyball players, but no biomechanical measurements were recorded. We found that biomechanical variables were poor at identifying symptomatic limbs despite good overall classification. We believe this is partly a consequence of the small number of symptomatic observations and that the VISA-P questionnaire score was not recorded for a specific limb. In addition, we noted that the trend for knee flexion at IC in symptomatic limbs conflicted with PTA limbs. This highlighted previously reported discordance between symptoms and PTA, which was confirmed on conventional US and MRI.[17,18] Generally, the regression models were more accurate in identifying limbs without PTA. This echoed a similar finding in a comparative clinical study that also concluded that combined metrics (athlete pain history, functional pain, VISA-P) more accurately identified PT.[16]

Early detection of clinically pertinent PT can lead to changes that improve athletic performance and enhance overall health and well-being. This work is novel and additive to the collective research relating patellar tendon pathology to baseline biomechanical landing and jumping patterns in the athletic preseason. Future work should focus on ways to detect clinically pertinent PT before it becomes deleterious. We strongly encourage prospective longitudinal assessment of imaging, symptoms, and biomechanical measurements across seasons. Kinematic and kinetic biomechanical measurements provide a layer of information that adds functional context and may help connect existing structural and symptom-related frameworks targeting PT. Quantitative biomechanics may be useful if incorporated into a multimodal functional screening tool to identify athletes at different levels of need for injury management, establish individual movement modification programs, or qualify imaging and symptoms to guide treatment decisions more efficiently. Larger samples must be collected, including controls, through multicenter collaboration. Functional tests should include land jumps at higher or multiple height levels, countermovement jumps, and movements with a lateral stop-jump component. In addition, female athletes and athletes at different levels of training, such as high school, collegiate, and recreational, are needed for better generalizability and risk modeling. Clinical data, such as pain and injury history, physical examination, and palpation pain mapping,[8] should also be collected. Last, other measurements must be explored in parallel with function; for example, electromyographic measurements and quantitative imaging can enhance identification and support validation of musculoskeletal models to investigate patellar tendon loading in detail.

Limitations

There are limitations to our study. A small sample size limited the power of the statistical analyses and the generalizability of results to other populations. This study was exploratory, and our analysis did not control for multiple comparisons, which increased the risk of a type I error. Our PTA variables were defined using imaging; therefore, we cannot directly link morphology findings to symptomatology. In addition, PTA observations included predominantly mild grades of tendon degeneration with fewer, more severe grades. Still, assuming that observed differences would be in the same direction irrespective of grade is reasonable. The analyses did not adjust for potential nontrivial dependencies between limbs within a subject and instead assumed independence. The 18-inch (45.7-cm) task height may not have been challenging enough to evoke more and greater biomechanical differences between limbs with and without PTA; the reported average standing vertical jump height of Division 1 NCAA athletes is 27 to 30 inches (68.6-76.2 cm), which also does not consider tucking the legs. Given that the task had an impact element, skin motion artifact was always present. Still, standard marker signal filtering methods were employed in a consistent manner to reduce this type of noise. Next, because the VISA-P data were not specific to an individual limb, the decision to assign one status to both limbs potentially mixed healthy and symptomatic limbs in the analyses. Last, given the prevalence of injuries in the sport, we recognize the exclusion of players who have had previous medical or surgical treatment.

CONCLUSION

Our findings suggest that biomechanical metrics may be used to characterize functional risk in a population

affected by PT. We quantified observable differences in land-jump biomechanics between limbs with and without PTA as seen on imaging and asymptomatic and symptomatic VISA-P scores. Biomechanical metrics successfully identified limbs without PTA but less successfully limbs with PTA. Common biomarkers included hip joint flexion, flexion velocities, and peak vertical limb loads.

ACKNOWLEDGMENT

The authors acknowledge Mandi Gibbons, Mehnaz Shahid, Bin Lin, Lydia Ko, and Emily Casaletto for their contributions to this study.

Supplemental Material for this article is available at https://journals.sagepub.com/doi/full/10.1177/23259671241242008#supplementary materials

REFERENCES

1. De Bleecker C, Vermeulen S, De Blaiser C, et al. Relationship between jump-landing kinematics and lower extremity overuse injuries in physically active populations: a systematic review and meta-analysis. *Sports Med*. 2020;50(8):1515-1532.
2. Decker MJ, Torry MR, Wyland DJ, Sterett WI, Richard Steadman J. Gender differences in lower extremity kinematics, kinetics and energy absorption during landing. *Clin Biomech (Bristol, Avon)*. 2003;18(7):662-669.
3. Dirrichs T, Quack V, Gatz M, et al. Shear wave elastography (SWE) for monitoring of treatment of tendinopathies: a double-blinded, longitudinal clinical study. *Acad Radiol*. 2018;25(3):265-272.
4. Drakos MC, Domb B, Starkey C, Callahan L, Allen AA. Injury in the national basketball association: a 17-year overview. *Sports Health*. 2010;2(4):284-290.
5. Edwards S, Steele JR, Cook JL, et al. Characterizing patellar tendon loading during the landing phases of a stop-jump task. *Scand J Med Sci Sports*. 2012;22(1):2-11.
6. Edwards S, Steele JR, McGhee DE, et al. Landing strategies of athletes with an asymptomatic patellar tendon abnormality. *Med Sci Sports Exerc*. 2010;42(11):2072-2080.
7. Hamill J, Palmer C, Van Emmerik RE. Coordinative variability and overuse injury. *Sports Med Arthrosc Rehabil Ther Technol*. 2012;4(1):45.
8. Hannington M, Tait T, Docking S, et al. Prevalence and pain distribution of anterior knee pain in collegiate basketball players. *J Athl Train*. 2022;57(4):319-324.
9. Harris M, Schultz A, Drew MK, et al. Thirty-seven jump-landing biomechanical variables are associated with asymptomatic patellar tendon abnormality and patellar tendinopathy: a systematic review. *Phys Ther Sport*. 2020;45:38-55.
10. Harris M, Schultz A, Drew MK, et al. Jump-landing mechanics in patellar tendinopathy in elite youth basketballers. *Scand J Med Sci Sports*. 2020;30(3):540-548.
11. Hernandez-Sanchez S, Hidalgo MD, Gomez A. Responsiveness of the VISA-P scale for patellar tendinopathy in athletes. *Br J Sports Med*. 2014;48(6):453-457.
12. Kregel J, van Wilgen CP, Zwerver J. Pain assessment in patellar tendinopathy using pain pressure threshold algometry: an observational study. *Pain Med*. 2013;14(11):1769-1775.
13. Lian OB, Engebretsen L, Bahr R. Prevalence of jumper's knee among elite athletes from different sports: a cross-sectional study. *Am J Sports Med*. 2005;33(4):561-567.
14. Major NM, Helms CA. MR imaging of the knee: findings in asymptomatic collegiate basketball players. *AJR Am J Roentgenol*. 2002;179(3):641-644.
15. Mann KJ, Edwards S, Drinkwater EJ, Bird SP. A lower limb assessment tool for athletes at risk of developing patellar tendinopathy. *Med Sci Sports Exerc*. 2013;45(3):527-533.
16. Mendonca Lde M, Ocarino JM, Bittencourt NF, et al. The accuracy of the VISA-P questionnaire, single-leg decline squat, and tendon pain history to identify patellar tendon abnormalities in adult athletes. *J Orthop Sports Phys Ther*. 2016;46(8):673-680.
17. Pappas GP, Vogelsong MA, Staroswiecki E, Gold GE, Safran MR. Magnetic resonance imaging of asymptomatic knees in collegiate basketball players: the effect of one season of play. *Clin J Sport Med*. 2016;26(6):483-489.
18. Peers KH, Lysens RJ. Patellar tendinopathy in athletes: current diagnostic and therapeutic recommendations. *Sports Med*. 2005;35(1):71-87.
19. Richards DP, Ajemian SV, Wiley JP, Zernicke RF. Knee joint dynamics predict patellar tendinitis in elite volleyball players. *Am J Sports Med*. 1996;24(5):676-683.
20. Rosso F, Bonasia DE, Cottino U, et al. Patellar tendon: from tendinopathy to rupture. *Asia Pac J Sports Med Arthrosc Rehabil Technol*. 2015;2(4):99-107.
21. Santana JA, Mabrouk A, Sherman A. Jumpers Knee. In: *StatPearls* [Internet]. StatPearls Publishing; 2020.
22. Scattone Silva R, Purdam CR, Fearon AM, et al. Effects of altering trunk position during landings on patellar tendon force and pain. *Med Sci Sports Exerc*. 2017;49(12):2517-2527.
23. Sprague AL, Smith AH, Knox P, Pohlig RT, Gravare Silbernagel K. Modifiable risk factors for patellar tendinopathy in athletes: a systematic review and meta-analysis. *Br J Sports Med*. 2018;52(24):1575-1585.
24. Tayfur A, Haque A, Salles JI, et al. Are landing patterns in jumping athletes associated with patellar tendinopathy? A systematic review with evidence gap map and meta-analysis. *Sports Med*. 2022;52(1):123-137.
25. Van der Worp H, de Poel HJ, Diercks RL, van den Akker-Scheek I, Zwerver J. Jumper's knee or lander's knee? A systematic review of the relation between jump biomechanics and patellar tendinopathy. *Int J Sports Med*. 2014;35(8):714-722.
26. Visnes H, Aandahl HA, Bahr R. Jumper's knee paradox—jumping ability is a risk factor for developing jumper's knee: a 5-year prospective study. *Br J Sports Med*. 2013;47(8):503-507.
27. Visnes H, Hoksrud A, Cook J, Bahr R. No effect of eccentric training on jumper's knee in volleyball players during the competitive season: a randomized clinical trial. *Clin J Sport Med*. 2005;15(4):227-234.
28. Vittinghoff E, McCulloch CE. Relaxing the rule of ten events per variable in logistic and Cox regression. *Am J Epidemiol*. 2007;165(6):710-718.
29. Woodley BL, Newsham-West RJ, Baxter GD. Chronic tendinopathy: effectiveness of eccentric exercise. *Br J Sports Med*. 2007;41(4):188-198.
30. Wu G, Siegler S, Allard P, et al. ISB recommendation on definitions of joint coordinate system of various joints for the reporting of human joint motion—part I: ankle, hip, and spine. International Society of Biomechanics. *J Biomech*. 2002;35(4):543-548.
31. Zaiontz C. *Real Statistics Resource Pack for Excel*. Version 7.9.1; 2021. www.real-statistics.com
32. Zwerver J, Bredeweg SW, van den Akker-Scheek I. Prevalence of Jumper's knee among nonelite athletes from different sports: a cross-sectional survey. *Am J Sports Med*. 2011;39(9):1984-1988.